RAILWAY TRANSPORT SYSTEM ENERGY FLOW OPTIMIZATION WITH INTEGRATED MICROGRID

Hrvoje Novak, Mario Vašak, Marko Gulin, Vinko Lešić

University of Zagreb, Faculty of Electrical Engineering and Computing, Unska 3, 10 000 Zagreb,
Laboratory for Renewable Energy Systems (url: www.lares.fer.hr),
hrvoje.novak@fer.hr, mario.vasak@fer.hr, marko.gulin@fer.hr, vinko.lesic@fer.hr

Abstract – Railway transport system microgrid model is observed from the point of balancing energy flows between accelerating and decelerating trains, hybrid energy storage systems and a single supply substation connected to the main power grid. In this paper, an energy flow optimization of a railway system microgrid is presented. Optimization problem is formulated as a linear program that takes into account energy storage systems with corresponding charge and discharge efficiencies, actual electricity prices and simulated daily train consumption profiles. Performance of the proposed approach is verified through one-day simulation scenario with model predictive control scheme and by considering different prediction horizon lengths.

1. Introduction

Transport systems are considered as large energy consumers that accounted for 31.8 % of overall energy consumption and for 1160.2 million tons of CO_2 emission in Europe in 2012 alone [1]. As a part of it, railway transport accounted for 2% of overall energy consumption and 7 million tons of CO_2 emission. For the same year in Croatia, 164.5 GWh were spent on transporting around 27.6 million passengers and 11 million tons of goods through the railway system [2]. Given the European Union climate and energy targets for 2020, also known as the 20-20-20 plan, it becomes important to improve the energy efficiency of the railway systems and market the "green image" of railway applications. Advances in information and communication technologies and electronics, together with more efficient and economically affordable energy storage systems, provide an opportunity for complex technical systems like railway transport to transform from passive loads that consume energy from the grid into more proactive entities with an ability to adapt to changing energy exchange terms and various demands of the power grid.

In order to increase the energy efficiency of the railway system, a considerable amount of effort is invested on better utilization and efficiency of braking trains regenerative energy [3]-[13]. Electric trains in braking convert the mechanical kinetic energy to electrical energy and feed it back to the catenary. If another train is accelerating while supplied from the same substation, energy sent back to the catenary will be used for powering its acceleration. If there are no accelerating trains nearby, regenerated energy causes overvoltage that potentially damages the system infrastructure. The energy is then dissipated on train built-in resistors, or it is stored in energy storage devices if available. An opportunity is provided to tune train timetables in order to closely coordinate nearby trains such that the braking trains regenerative energy is immediately reused by accelerating trains [3], [4]. Introduction of on-board and stationary energy storage systems [5]-[13] for storing the regenerative braking energy for later use show that savings of up to 30 % of regenerative energy are achievable. In order to further increase the economic effects related to energy flows of the railway system, it is necessary to implement a higher-level control system to take into account the possibility of different electricity prices throughout the day or changing acceptable power exchange levels imposed by the power utility.

The concept of microgrids brought possibility of dynamical optimization of the railway system total power consumption by means of distributed regenerative braking, renewable energy sources and storages, all of which transforms it to active participant in the power system [8], [9]. A clear microgrid structure is formable for each railway system supply substation, where braking trains present distributed sources and the energy storage systems are installed in the substation. The microgrid energy management system balances the energy flows between accelerating trains energy consumption, decelerating trains energy production, energy storages and energy exchange with the grid. It takes into account declared price profile for energy exchange on the grid side, current state of the energy storage and prediction of trains energy consumption, and makes the decision when to buy/sell electrical energy from/to the utility grid and in which amount. Therefore each supply substation along the train route may be observed as an individual microgrid. By making a step-up further, the railway traffic system is observed as a chain of microgrids that can be coordinated in order to attain minimum cost for energy drawn from the grid while all the trains operate according to timetable and operational constraints along the routes.

Previous work on microgrid energy flow optimization is performed on a DC microgrid that consists of photovoltaic array, batteries stack and fuel cells stack with electrolyser, all connected to the grid via bidirectional power converter. Minimization of microgrid operating costs is formulated by using a linear program that takes into account energy storage devices charge and discharge efficiencies [14], [15].

The improvement in energy consumption efficiency has additional advantages for the railway operator and the power system in general: the use of the grid is more efficient and a smaller capacity is required; the railway operator becomes less dependent on the power grid; decentralization of the power system thus increasing its reliability and stability; finally, the amount of power that needs to be contracted is

reduced and the operating costs are further decreased [4].
In this paper, a railway system microgrid is considered consisting of a hybrid energy storage system, distributed generation of nearby trains in braking and a bidirectional connection to the power grid through a supply substation. Microgrid energy flow optimization problem is defined as a linear program (LP) and a model predictive control (MPC) scheme with receding horizon philosophy is implemented. The performance of the proposed approach is verified on a one-day simulation scenario considering different prediction horizon lengths.
This paper is structured as follows. In Section 2, a microgrid model is presented. In Section 3, the optimization problem and model predictive control scheme are formulated. Performance verification of the proposed approach is given in Section 4.

2. Microgrid model

The microgrid model, presented in Fig. 1, is observed from the point of balancing energy flows between accelerating and decelerating trains, hybrid energy storage system and a supply station connected to the utility grid with variable energy price c. Considering a hierarchical design of microgrid control, the focus here is put on high-level optimization of energy flows, whereas voltage stability and power quality are controlled at lower control levels [15].

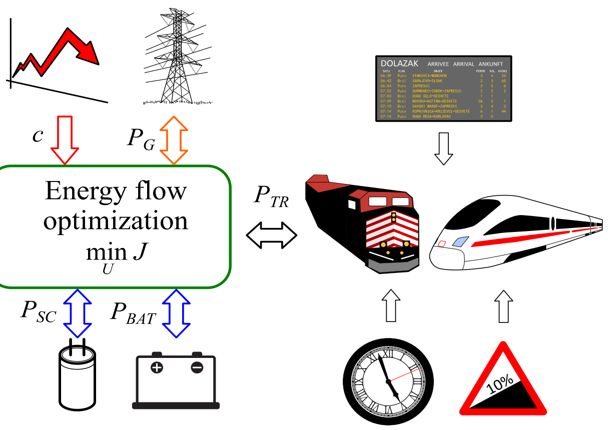

Fig. 1 – Energy flow optimization problem illustration.

Table 1 – Microgrid components

Component	Notation	Rated power
Grid connection	P_G	15 MW
Supercapacitor	P_{SC}	1.2 MW
Battery storage	P_{BAT}	0.3 MW
Train traction power	P_{TR}	13 MW
Power burned in the resistors	P_R	15 MW

The following balance equation in the microgrid is always satisfied:

$$P_{TR} + P_R = P_G + P_{SC} + P_{BAT}, \qquad (1)$$

where P_{TR} denotes the power consumption ($P_{TR} > 0$) or production ($P_{TR} < 0$) by accelerating/decelerating trains and P_R is the excess power than can not be exported to the utility grid and is burned on the trains resistors ($P_R \geq 0$). By convention, power components P_{SC}, P_{BAT}, and P_G are positive when supplying power to the microgrid. Therefore, power components P_{SC} and P_{BAT} are negative for charging, and power component P_G is negative for exporting energy to the utility grid. Power component P_R is positive, denoting the power taken from the microgrid.

A. Energy storage systems

Microgrid energy storage system is chosen as hybrid storage system consisted of supercapacitors and batteries. The use of hybrid storage devices ensures the storage flexibility, where the usage of supercapacitors is essential to capture the high power density and high frequency of operation associated to regenerative braking; the usage of batteries for absorbing this short peaks of energy entails an oversized system and short life cycle. On the other hand, batteries are characterised with high energy density and an ability to provide storage for larger period of time. Hybrid solution is a reasonable balance between the two [5], [6], [10].
Considered energy storage systems are modelled with discrete-time first-order difference equations [14], [15]:

$$\begin{cases} x_{k+1}^{BAT} = x_k^{BAT} - \dfrac{\Delta T}{C^{BAT}}\left(\dfrac{1}{\eta_{dch}^{BAT}} P_{dch,k}^{BAT} + \eta_{ch}^{BAT} P_{ch,k}^{BAT}\right), \\ x_{k+1}^{SC} = x_k^{SC} - \dfrac{\Delta T}{C^{SC}}\left(\dfrac{1}{\eta_{dch}^{SC}} P_{dch,k}^{SC} + \eta_{ch}^{SC} P_{ch,k}^{SC}\right), \end{cases} \qquad (2)$$

where k denotes discrete time instant, state x_k is normalized state-of-charge (SoC), C is storage capacity, η_{ch} and P_{ch} are charging efficiency and charging power component of storage system ($P_{ch} \leq 0$), while η_{dch} and P_{dch} are discharging efficiency and discharging power component of storage system ($P_{dch} \geq 0$). Sampling time ΔT is chosen to be 15 seconds in order to match the precomputed train consumption profile resolution obtained from [16], where ΔT is chosen to capture the train dynamics and avoid the linearization effects. Power ratings of involved microgrid components are listed in Table 1, while parameters of the considered storage systems are listed in Table 2.

Table 2 – Energy storage system parameters

Parameter	Battery storage	Supercapacitor
Capacity [kWh]	60	13
Discharge efficiency	0.8	0.95
Charge efficiency	0.8	0.95
Maximum SoC	1	1
Minimum SoC	0.1	0.1

The discrete-time energy storage system model (2) can be rewritten in state-space form:

$$x_{k+1} = Ax_k + Bu_k, \qquad (3)$$

where A is identity matrix I_{2x2}, B^{2x4} is the system input matrix calculated from (2), $x_k = [x_k^{BAT}, x_k^{SC}]^\top$ state vector and u_k is $\left[P_{dch,k}^{BAT}, P_{ch,k}^{BAT}, P_{dch,k}^{SC}, P_{ch,k}^{SC}, P_k^R\right]^\top$.

B. Train traction power

Train traction power profile P_{TR} is obtained as a precomputed solution to the optimization problem presented in [16], [17], where trains on route energy consumption profile was minimized with respect to time-tables, route restrictions (speed limits, train traction force boundaries) and passengers comfort. The train optimal control problem was solved for travel durations of 5, 10 and 15 minutes (between two adjacent stations) and solutions are merged to form a vector of optimum power consumption profile for each 15 seconds time instant over the period of next 24 hours. Exemplary on-route passenger train consumption profiles for 5, 10 and 15 minutes travel time between the two stations are presented in Fig. 2.

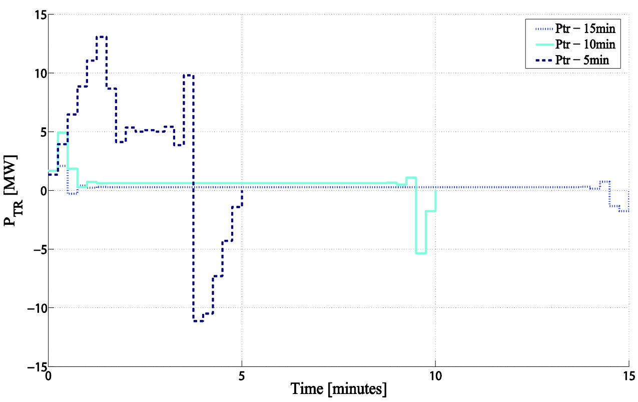

Fig. 2 – Train consumption profiles between two stations.

C. Utility grid connection

Connection to the grid is established through a bidirectional traction substation with nominal power P_G chosen to match the most common type of supply substations found in railway systems in Croatia. Electricity price profiles c_k for the simulation period are obtained from European power exchange site [13] that accounts for more than a third of total European power consumption. For simplicity, same prices are assumed for buying and selling energy from the grid.

Since the simulated train nominal power is in a megawatt scale, renewable energy sources like photovoltaic panels or wind turbines are not considered because of a rather small power production contribution in comparison to the train consumption. Therefore, only power generation in the microgrid is the regenerative braking energy from trains.

3. Energy flow optimization

The objective of the energy flow optimization is set to minimize the economic cost of the microgrid operation, taking into account the current SoC of the microgrid storages x_0, predicted trains consumption profile, electricity price profile c_k representing the economic criterion of the utility grid and technical constraints on microgrid components. Energy flow optimization results in optimal charging/discharging profiles for storage components, $P_{dch,k}^{BAT}$, $P_{ch,k}^{BAT}$, $P_{dch,k}^{SC}$ and $P_{ch,k}^{SC}$ that guarantee the optimal economic cost on the prediction horizon N, and P_k^R which ensures that no excess power is exported to the utility grid, where $0 \leq k \leq N-1$ [15].

The objective function is formulated as follows:

$$J = \sum_{k=0}^{N-1} c_k P_k^G \Delta T, \tag{4}$$

where N is prediction horizon length, c_k is the electricity price for time instant k expressed in €/MWh, P_k^G is the utility grid power component determined by balance equation (1), which represents the total power exchanged with the grid. It is important to notice that the criterion (4) is a function only of exchanged energy on the prediction horizon under certain price conditions.

For simplicity, the consumption of auxiliary power supplies in trains or the efficiency of the traction power converters are omitted. Microgrid physical constraints are introduced to the control problem as state and input constraints. Constraints include supercapacitor and battery SoC limitations in order to preserve the health of the storage systems:

$$x_{SC,min} \leq x_{SC} \leq x_{SC,max}, \tag{5}$$
$$x_{BAT,min} \leq x_{BAT} \leq x_{BAT,max}, \tag{6}$$

maximum charging and discharging power of the supercapacitor and batteries:

$$P_{dch,min}^{BAT} \leq P_{dch}^{BAT} \leq P_{dch,max}^{BAT}, \tag{7}$$
$$P_{ch,min}^{BAT} \leq P_{ch}^{BAT} \leq P_{ch,max}^{BAT}, \tag{8}$$
$$P_{dch,min}^{SC} \leq P_{dch}^{SC} \leq P_{dch,max}^{SC}, \tag{9}$$
$$P_{ch,min}^{SC} \leq P_{ch}^{SC} \leq P_{ch,max}^{SC}. \tag{10}$$

Constraints on utility grid power rating are defined as follows:

$$P_{G,min} \leq P_G \leq P_{G,max}, \tag{11}$$

and constraints on the power dissipated in the resistors:

$$P_R \geq 0. \tag{12}$$

After the objective function (4) and the constraints (5)-(12) have been defined, the optimization problem is formulated as a linear program written in the following matrix form:

$$\begin{aligned} &\min_{\boldsymbol{u}} J(\boldsymbol{u}, x_0, \boldsymbol{c}, \boldsymbol{P}_{TR}) = \boldsymbol{f}^{\top}\boldsymbol{u} + d, \\ &s.t.\ \boldsymbol{E}_u \boldsymbol{u} \leq \boldsymbol{E}_x x_0 + \boldsymbol{g}, \end{aligned} \tag{13}$$

where vectors $\boldsymbol{f}$ and $\boldsymbol{g}$, matrices $\boldsymbol{E}_u$ and $\boldsymbol{E}_x$ and constant d are calculated from (4)-(12). Trains energy consumption vector $\boldsymbol{P}_{TR}$ is precalculated. Solution of the described optimization problem is a vector of optimum values of control variables $\boldsymbol{u}^*$ over the horizon N. However, during the time from which the control variables are calculated to the end of the prediction horizon, several disturbances may act on the system and calculated solution may no longer be optimal.

Therefore a Model Predictive Control (MPC) scheme [19] is introduced with receding horizon philosophy for closed-loop control, presented in Fig. 3. In MPC framework, the optimal control sequence $\boldsymbol{u}^*$ for the prediction horizon N is calculated at time $t = 0$ by solving the energy flow optimization problem (13) for the initial state of the system $x_0 = x(t)$. In the receding horizon philosophy only the first control action $u(t) = \boldsymbol{u}_0^*$ is implemented and the system is propagated to the state at time instant $t + 1$ where the optimization problem is again solved for newly defined circumstances. The optimization problem uses a system model formulated in (3) to simulate the system behaviour on the prediction horizon. Due to model inaccuracy or different disturbances that may act on the system during that time, the optimal control sequence is again recalculated at time $t + 1$ to compensate for any unpredicted system behaviour. By recalculating the optimal control sequence at each time instant t with all the pricing and consumption information currently available and only implementing the first control vector, feedback is introduced through system states $x(t)$.

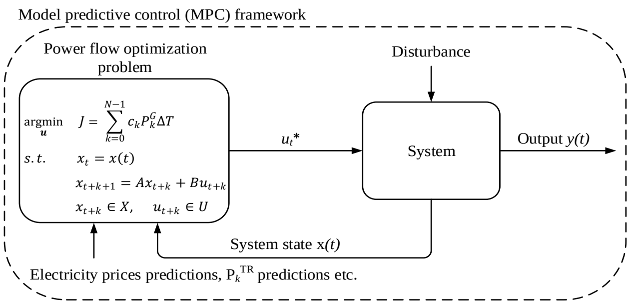

Fig. 3 – Model predictive control framework.

4. Results

Performance of the proposed approach in this paper is verified with a simulation scenario based on actual electricity price data (Epex prices for 16th and 17th of July 2015 [18]), train consumption profiles obtained from the optimization problem presented in [16], and a model of hybrid energy storage system consisted of supercapacitors and batteries. The system is simulated with a time step ΔT of 15 seconds and the optimal energy flows are calculated for a period of 24 hours since energy prices are usually given one day in advance. The procedure is studied for different lengths of the prediction horizon N.

Daily economic cost of the railway system operation with integrated microgrid is formulated in 15 seconds scale as:

$$c_{cost} = \sum_{t=0}^{5760} c(t) P_G(t) \Delta T, \tag{14}$$

where t ranges to 24 hours ($5760 \cdot 15s = 24h$) and P_G is formulated in (1). It is assumed that only 3 MW of regenerative power can be exported to the utility grid, therefore, $P_{G,min}$ is set to -3 MW in (11). Solution obtained through optimizing microgrid energy flows is compared with a railway system operation cost without the integrated microgrid, in which case $P_G(t) = P_{TR}(t) + P_R(t)$ in (14), where $P_R(t)$ is set to ensure that $P_G(t) \geq -3$ MW, meaning that only the cost of trains consumption without the excess regenerative braking power is taken into account for calculating the daily economic cost of railway system operation. Total operation cost of the railway system without integrated microgrid amounts to 327.66 €, with 60 % of the regenerative energy exchanged with the grid.

Linear optimization problem formulated in (13) is solved using IBM ILOG CPLEX 12.6. optimization package, while the MPC closed loop control scheme is implemented using YALMIP toolbox for MATLAB [20].

Operation costs of the railway system with integrated microgrid are presented in Table 3 and compared with the railway system operation costs.

Table 3 – Railway system operation costs for one-day period

Prediction horizon *N* [h]	**1**	**2**	**3**
Operation costs c_{cost} [€]	316.18	316.09	315.91
Improvement	11.48 € 3.50 %	11.57 € 3.53 %	11.75 € 3.58 %
Prediction horizon *N* [h]	**6**	**12**	**24**
Operation costs c_{cost} [€]	315.77	315.92	315.92
Improvement	11.89 € 3.63 %	11.74 € 3.58 %	11.74 € 3.58 %

Optimizations performed with shorter prediction horizons are outperformed by the ones with longer prediction horizons due to the fact that the control algorithm is able to find the highest prices in a longer time period and therefore better utilize stored energy by discharging the storage system during the highest price on the horizon. Although it was expected that the best performance are obtained for $N = 24\ h$, due to specific price and consumption profiles, the best results are obtained for $N = 6\ h$.

In Fig. 4, daily microgrid operation is presented including (i) energy storage charging and discharging profiles – optimal control sequence, (ii) electricity price profile, (iii) grid and train consumption profiles, and (iv) energy storage SoC profiles, with sampling time of 15 seconds throughout 24 hours, where N is set to 6 hours as it is shown to be the best scenario in Table 3.

A closer view of the control system behaviour is shown in Fig. 5, where results of one hour system performance are presented (time period of 17:00-18:00 h).

From the presented results it is observed that energy storage is discharged during low electricity prices and charged during high electricity prices. It is shown that due to limitation of the power that can be exported to the grid, supercapacitors are mainly charged during the braking of trains in order to utilize the regenerative braking energy which confirms the choice of a hybrid energy storage systems since batteries are rarely used for storing the regenerative braking energy and are better exploited for utilization of the difference in electricity price profile throughout the day.

Increase in the energy storage capacity (C^{BAT}, C^{SC}) ensures further reductions of the operation costs since more of the regenerative braking energy is stored in the storage rather than dissipated in the resistors. However, an increase in the capacity would have a significant impact on the investment costs of the storage system. To find the optimal capacity of the storage system, a cost-benefit analysis should be performed taking into account the investment costs and the reduction of the operational costs.

Railway system with integrated microgrid restored 71 % of the regenerative braking energy. Additional simulations were performed with the prediction horizon $N = 6$ to measure the control system performance for different limitations on the power exported to the grid $P_{G,min}$, with results presented in Table 4. It is shown that the performance of the control system compared to the no-microgrid behaviour is decreased when more regenerative braking energy can be exported to the grid.

Table 4 – Operation costs with respect to $\boldsymbol{P_{G,min}}$

Maximum exported power to the grid $P_{G,min}$ [MW]	**-3**	**-5**	**-15**
Operation costs without microgrid [€]	327.6	308.2	287.2
Operation costs with microgrid [€]	316.2	301.1	285.8
Improvement [%]	3.50	2.32	0.47
Restored regenerative energy without microgrid [%]	58.86	78.22	100
Restored regenerative energy with microgrid [%]	71.67	85.46	100
Improvement [%]	12.81	7.24	0

5. Conclusion

In this paper energy flow optimization in railway system with integrated microgrid is presented. Model predictive control scheme is implemented and the approach is verified for different prediction horizon lengths on a simulation scenario. It is shown that the proposed approach reduces the railway system operation costs through charging and discharging of the hybrid energy storage system, with better performance for longer prediction horizons. Choice of energy storage systems is validated as it is shown that supercapacitors are used for storing the regenerative braking energy, while batteries perform better at utilization of the difference in the electricity price profile throughout the day. Due to inherent complexity, the railway system is observed from two different control levels. The higher-level railway system optimization introduced here optimizes energy flows with respect to external grid conditions, state of the energy storage system and railway traffic. Lower, consumption level optimization, where each train is controlled to achieve least travel costs while maintaining the time-table and passengers comfort can be recomputed such that interaction of both levels is taken into account and the computed energy consumption profile on the lower level directly maximizes the global economic gain of the whole system operation. Price of energy exchange with the grid is for an individual train transformed through the higher coordination system and the economic cost is reduced by cooperative action of all the trains in balancing energy flows.

Acknowledgments

This work has been fully supported by Croatian Science Foundation under the project No. 6731 (project 3CON – Control-based Hierarchical Consolidation of Large Consumers for Integration in Smart Grids, www.fer.unizg.hr/3con).

References

[1] Publications Office of the European Union, *European Commission. EU Transport in figures: Statistical pocketbook 2014.* Luxembourg, 2014.

[2] “Annual energy report – Energy in Croatia 2013”, Republic of Croatia, Ministry of economy, December 2014., Zagreb

[3] X. Sun, H. Cai, X. Hou, M. Zhang and H. Dong, “Regenerative Braking Energy Utilization by Multi Train Cooperation,” *Intelligent Transportation Systems (ITSC), 2014 IEEE 17th International Conference on*, pp.139-144, Oct. 2014.

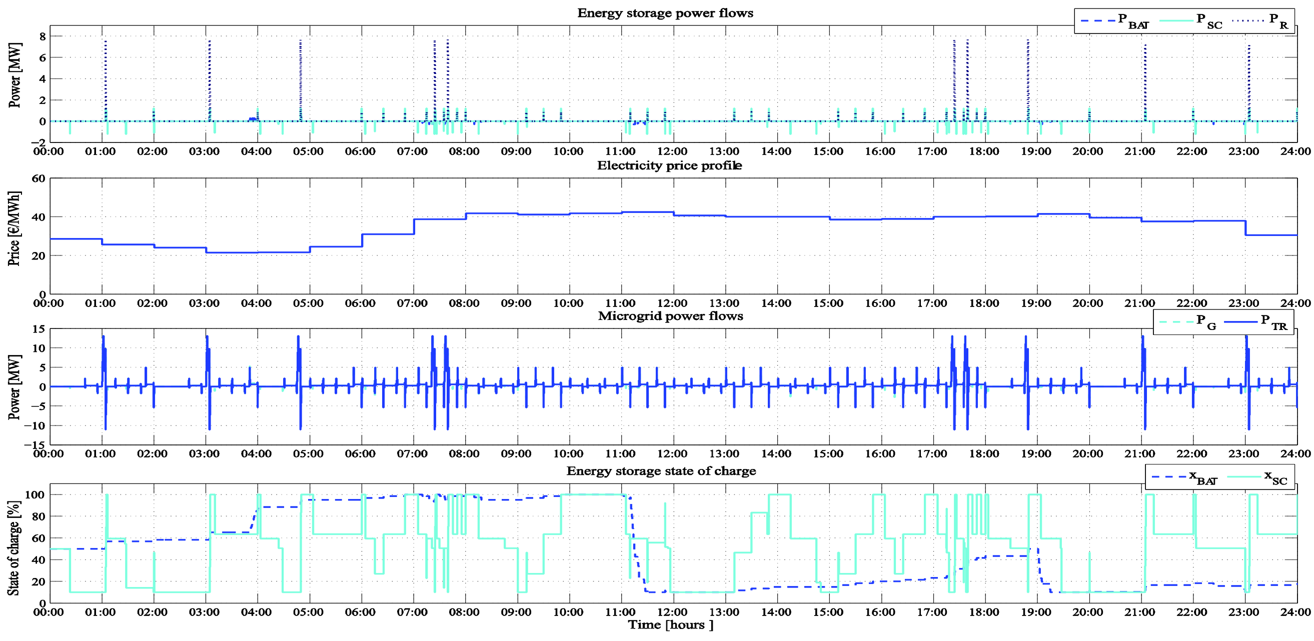

Fig. 4 – Energy flow optimization results for 24 hours period with N= 1440 (6h).

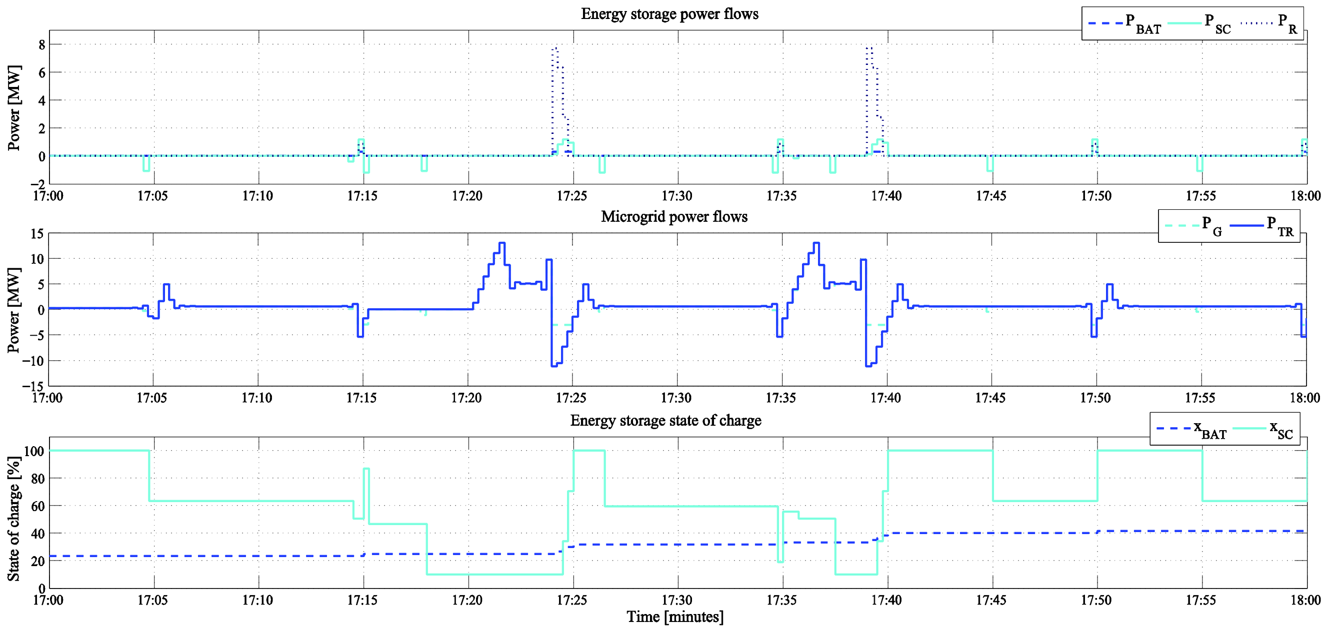

Fig. 5 – Energy flow optimization results for 1 hour period with N= 1440 (6h).

[4] S. Su, T. Tang, C. Roberts and L. Huang, "Cooperative train control for energy-saving," *Intelligent Rail Transportation (ICIRT), 2013 IEEE International Conference on*, pp.7-12, Aug. 2013.

[5] S. de la Torre, A. J. Sanchez-Racero, J. A. Aguado, M. Reyes and O. Martinez, “Optimal Sizing of Energy Storage for Regenerative Braking in Electric Railways Systems,” *Power Systems, IEEE Transactions on*, vol. 30, no. 3, pp. 1492-1500 May 2015.

[6] Y. Jiang, J. Liu, W. Tian, M. Shahidehpour and M. Krishnamurthy, "Energy Harvesting for the Electrification of Railway Stations: Getting a charge from the regenerative braking of trains," *Electrification Magazine, IEEE* , vol. 2, no. 3, pp. 39-48 Sept. 2014.

[7] E. P. de la Fuente, S. K. Mazumder and I. G. Franco, "Railway Electrical Smart Grids: An introduction to next-generation railway power systems and their operation.," *Electrification Magazine, IEEE*, vol. 2, no. 3, pp. 49-55 Sept. 2014.

[8] P. Pankovits, J. Pouget, B. Robyns, F. Delhaye and S. Brisset, "Towards railway-smartgrid: Energy management optimization for hybrid railway power substations," *Innovative Smart Grid Technologies Conference Europe (ISGT-Europe), 2014 IEEE PES*, pp.12-15 Oct. 2014.

[9] S. Nasr, M. Iordache and M. Petit, "Smart micro-grid integration in DC railway systems," *Innovative Smart Grid Technologies Conference Europe (ISGT-Europe), 2014 IEEE PES*, pp. 12-15 Oct. 2014.

[10] T. Ratniyomchai, S. Hillmansen and P. Tricoli, "Recent developments and applications of energy storage devices in electrified railways," *Electrical Systems in Transportation, IET*, pp. 9-20 March 2014.

[11] A. Okui, S. Hase, H. Shigeeda, T. Konishi and T. Yoshi, "Application of energy storage system for railway transportation in Japan," *Power Electronics Conference (IPEC), 2010 International*, pp. 3117-3123 June 2010.

[12] H. Hayashiya, S. Kikuchi, K. Matsuura, M. Hino, M. Tojo, T. Kato, M. Ando, T. Oikawa, M. Kamata and H. Munakata, "Possibility of energy saving by introducing energy conversion and energy storage technologies in traction power supply system," *Power Electronics and Applications (EPE), 2013 15th European Conference on*, pp. 2-6 Sept. 2013.

[13] V. Calderaro, V. Galdi, G. Graber and A. Piccolo, "Siting and sizing of stationary SuperCapacitors in a Metro Network," *AEIT Annual Conference, 2013*, pp. 3-5 Oct. 2013.

[14] M. Gulin, J. Matuško and M. Vašak, "Stochastic model predictive control for optimal economic operation of a residential DC microgrid," *Industrial Technology (ICIT), 2015 IEEE International Conference on*, pp.505-510 March 2015.

[15] M. Gulin, M. Vašak and M. Baotić, “Analysis of microgrid power flow optimization with consideration of residual storages state,” *Proceedings of the 2015 European Control Conference*, Austria, pp. 3131-3136.

[16] M. Vašak, M. Baotić, N. Perić, and M. Bago, “Optimal rail route energy management under constraints and fixed arrival time,” in *Proceedings of the European Control Conference*, 2009, pp. 2972–2977.

[17] M. Vašak, M. Baotić, M. Bago, and N. Perić, “Constrained energy optimal control of trains: Conceptual implementation,” in *30th Conference on Transportation Systems with International Participation Automation in Transportation*, 2010, pp. 143–146.

[18] EPEX SPOT. (2015, July 18). European Power Exchange Electricity Index. Available: http://www.epexspot.com

[19] J. B. Rawlings and D. Q. Mayne, *Model Predictive Control: Theory and Design*, 1st ed. Nob Hill Publishing, 2009.

[20] J. Löfberg, “YALMIP: A toolbox for modelling and optimization in MATLAB,” in *Proceedings of the 2004 IEEE International Symposium on Computer Aided Control System Design*, Taiwan, 2004, pp. 284–289.